Nonlinear Control of an Inverted Pendulum

Daniel Bodily, Patrick Taylor

April 13, 2016

1 Introduction

The inverted pendulum is a canonical control problem that has merited much attention in classical system dynamics literature due to its highly unstable equilibrium point and relatively simple, nonlinear model. The problem consists of a rod of length L_1 and mass m_1 attached to a cart of mass m_0. The cart is free to slide along a frictionless rail. The controller outputs a desired force exerted horizontally on the cart and the objective is to successfully balance the inverted pendulum in its vertical position while regulating the position of the cart to a set location. The double inverted pendulum is an extension of this problem, with a second rod of mass m_2 and length L_2 attached to the end of the first pendulum. The system is shown in figure 1. Despite it's relatively simple model, the inverted pendulum is an inherently unstable system and sophisticated control designs must be carefully applied to successfully balance the pendula in its upright position.

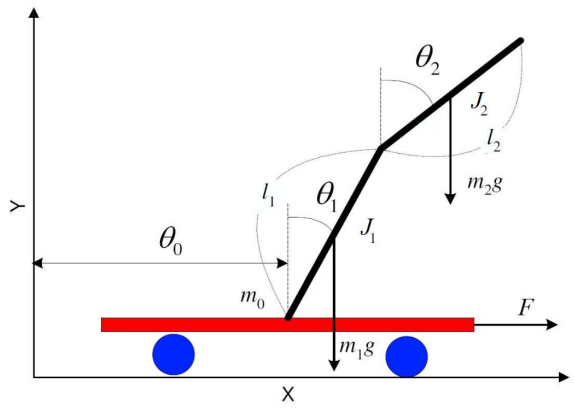

Figure 1: Nonlinear MPC applied to a double inverted pendulum system.

2 Background

As the inverted pendulum continues to provide a benchmark test to many nonlinear control strategies, the theory behind the derivation of its model has been adequately explored in many references. In the development of the model and control used in this paper, two particular articles proved most useful [1], [2].

Jadlovska et. al. in [1] uses the *Inverted Pendula Model Equation Derivator* (a MATLAB application) to efficiently generate a model of the double inverted pendulum system. This application uses a generalization of Lagrangian dynamics (applied to *n-link* systems) that automatically produces models for a user-chosen type of system.

This work also demonstrates the effectiveness of several matlab applications in applying linear state feedback control to the inverted pendula system. It also highlights the degree of difficulty present in controlling this highly nonlinear system. While the cart's position is shown to be effectively controllable, the inverted pendula frequently fall out of their desired trajectories around the desired unstable equilibrium point.

Nalavade et. al. in [2] also uses Lagrangian dynamics to develop a nonlinear model of the double inverted pendulum system. These equations are then linearized the system around its unstable equilibrium and applies LQR to successfully balance both pendula in their upright position. It is unclear however how this method would perform under the presence of disturbances. Friction at the joints and on the cart rail is also not handled in this model.

3 Model Development

The model we employ is presented in [1] and is given as:

$$\begin{bmatrix} m_o+m_1+m_2 & (\frac{1}{2}m_1l_1+m_2l_1)cos\theta_1(t) & \frac{1}{2}m_2l_2cos\theta(t) \\ (\frac{1}{2}m_1l_1+m_2l_1)cos\theta_1(t) & J_1+m_2l_1^2 & \frac{1}{2}m_2l_1l_2cos(\theta_1(t)-\theta_2(t)) \\ \frac{1}{2}m_2l_2cos\theta_2(t) & \frac{1}{2}m_2l_1l_2cos(\theta_1(t)-\theta_2(t)) & J_2 \end{bmatrix} \begin{bmatrix} \ddot{\theta}_0(t) \\ \ddot{\theta}_1(t) \\ \ddot{\theta}_2(t) \end{bmatrix} +$$

$$\begin{bmatrix} \delta_0 & -(\frac{1}{2}m_1l_1+m_2l_1)\dot{\theta}_1sin\theta_1(t) & \frac{1}{2}m_2l_2cos\theta_2(t) \\ \frac{1}{2}m_1l_1cos\theta_1(t) & \delta_1+\delta_2 & -\delta_2-\frac{1}{2}m_2l_1l_2\dot{\theta}_2sin(\theta_1(t)-\theta_2(t)) \\ \frac{1}{2}m_2l_2cos\theta(t) & -\delta_2-\frac{1}{2}m_2l_1l_2\dot{\theta}_2sin(\theta_1(t)-\theta_2(t)) & \delta_2 \end{bmatrix} \begin{bmatrix} \dot{\theta}_0(t) \\ \dot{\theta}_1(t) \\ \dot{\theta}_2(t) \end{bmatrix} +$$

$$\begin{bmatrix} 0 \\ -(\frac{1}{2}m_1+m_2)gl_1sin\theta_1(t) \\ -(\frac{1}{2}m_2gl_2sin\theta(t) \end{bmatrix} = \begin{bmatrix} F(t) \\ 0 \\ 0 \end{bmatrix}$$

where m_0 is the mass of the cart,m_1 and m_2, l_1,l_2 are the masses and lengths of pendula respectively, δ_0 is the friction coefficient of the cart on the rail, δ_1, δ_2 are the damping constants at the joints of the pendula, $J_1 = \frac{1}{3}m_1l_1^2$, $J_2 = \frac{1}{3}m_2l_2^2$ are the moments of inertia about the joints and $F(t)$ is the input force given by the controller. The state variables of the equation are θ_0, the horizontal position of the cart and θ_1,θ_2 are the angles of the pendula

with respect to their downwards position. These relationships are depicted in figure 1.

4 Simulation Results

Figure 2 shows a simulation of dropping both pendula from 179 degrees from the downward position. Parameters for this simulation are given as $m_0 = 3kg$, $m_1 = m_2 = 2.75kg$, $l_1 = l_2 = .5m$, $\delta_0 = \delta_1 = \delta_2 = .1.2kgm^2s^{-1}$.

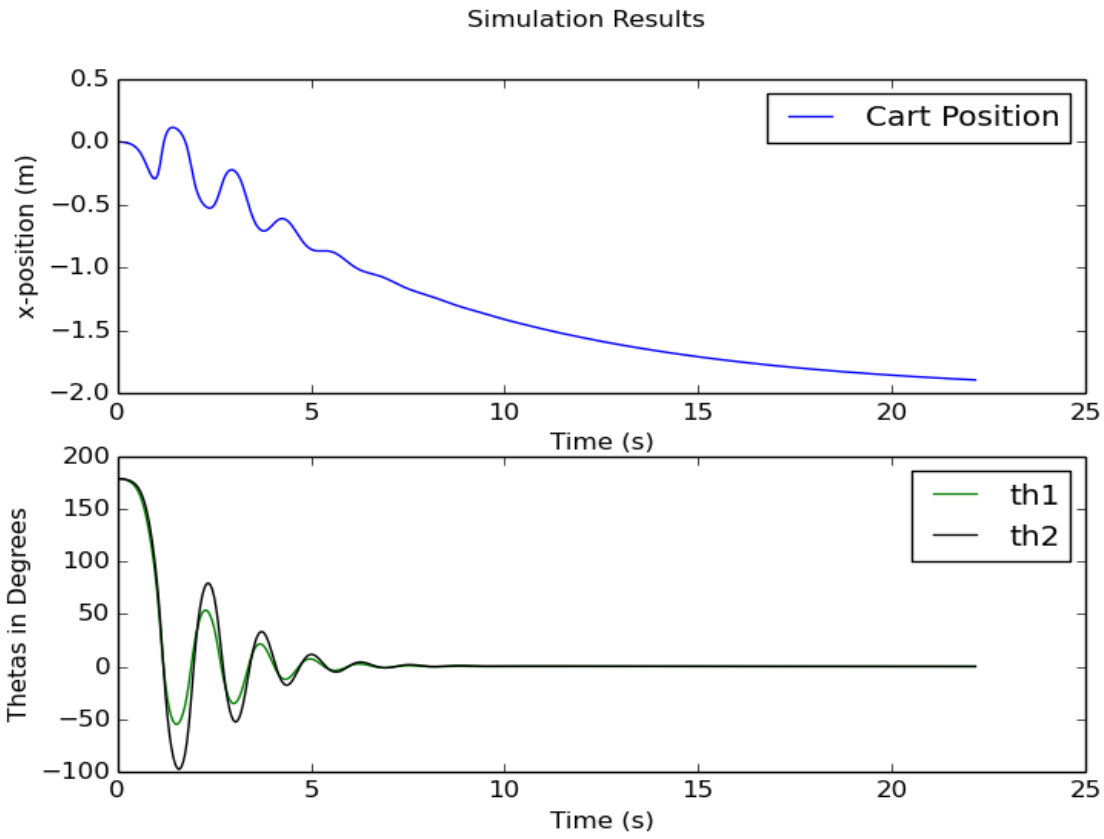

Figure 2: The double pendula system dropped with initial conditions $\theta_0 = 0$, $\theta_1 = \theta_2 = 179 * \pi/180$ deg.

The cart moves in phase with the pendula and both angles converge to zero in around 7 seconds. These simulation results are satisfactory in demonstrating the utility of the model

equations given previously as well as the capability of this model for control. We noticed in performing our simulations that the solver performed very poorly in cases where the damping coefficients δ_i were orders of magnitude smaller than the masses. This arises from poorly conditioned matrices around equilibrium points where $\dot{\theta}_1 = \dot{\theta}_2 = \theta_1 = \theta_2 = 0$. To keep this error from arising in estimation and control, we are careful to choose reasonable damping parameters that stabilize the system.

5 Moving Horizon Estimation (MHE)

We now assume the masses of the same system examined earlier are unknown (though assumed to be between 1 and 10 kg.) and implement a moving horizon estimator (MHE) run at 10 Hz to approximate these masses. The MHE looks back 1.2 seconds in the simulation and seeks to match predicted and measured values of the carts position. Measured values are obtained by adding Gaussian noise to the simulated cart's position, demonstrating the MHE's robustness to sensor noise. The estimator's weighting on measurements is approximately 10x that of model values and a squared error norm objective function is used in the estimation.

APMonitor		Objective	CV(1)	SV(1)	SV(2)
	Sensitivities	Function	p(10).n(3).x1	p(10).n(3).th1	p(10).n(3).th2
FV(1)	p(1).n(1).m1	-9.406E-09	5.527E-03	-2.349E-03	2.528E-04
FV(2)	p(1).n(1).m2	1.955E-08	-9.844E-03	-2.003E-03	-3.221E-04
MV(1)	p(1).n(1).f	5.118E-04	4.067E-03	1.770E-03	2.759E-03

Figure 3: Sensitivities of the MHE near the end of the simulation demonstrating that the estimator has converged on masses m_1 and m_2.

We initialize θ_1 and θ_2 at 50° and 0° respectively and the horizontal position at zero. The pendula are then released and allowed to settle to their equilibrium positions with no input force being applied. Figure 3 shows sensitivities of the objective function to changes in the estimated masses. At the end of the estimation routine these sensitivities are approximately zero, demonstrating the estimator has converged on accurate estimates of the masses. Figure 4 shows that over a period of about 4 seconds, the estimator is successful in closely approximating the masses of the system. Final estimates of the masses were reported at $\hat{m}_1 = 2.8kg$ and $\hat{m}_2 = 2.97kg$.

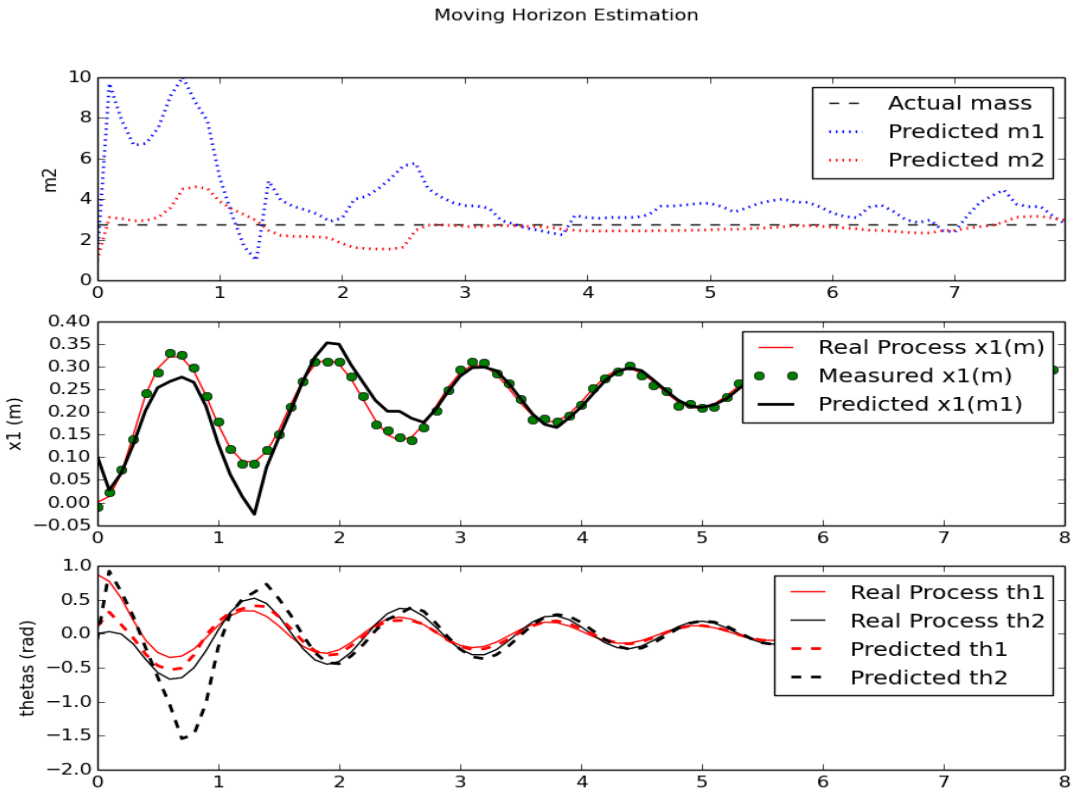

Figure 4: The double pendula system dropped with initial conditions $\theta_1 = 50$, $\theta_1 = 50\pi/180, \theta_2 = 0\,\text{deg}$. The MHE successfully converges on masses that match measured and model values.

6 Model Predictive Control (MPC)

MPC utilizes the nonlinear dynamic equations directly to formulate an optimization problem over a horizon $H = t_i, t_{i+1}...t_{i_n}$. At each time step, the controller searches for an optimal control sequence $u_i, u_{i+1}...u_{i_n}$ that will drive the states to their desired set points.

For convenience, we define two additional variables,

$$C_1 = 1 + cos(\theta_1) \tag{1}$$

$$C_2 = 1 + cos(\theta_2) \tag{2}$$

We then design a model predictive controller (MPC) that seeks an optimal input sequence to drive C_1 and C_2 to zero (pendula pointed upwards). We define a squared error objective function in (3) with $C_1^d = C_2^d = 0$ with equal weightings placed on both states.

$$\begin{aligned} &\underset{u_i, u_{i+1}...u_n}{\text{argmin}} && \phi(x) = (\chi - \chi_d)^T W_t (\chi - \chi_d) + \delta u^T c_{\delta u} \\ &\text{subject to dynamic eqs.} \end{aligned} \tag{3}$$

We set the cost on changing the input to be $c_{\delta u} = 10^{-5}$ and define an upper and lower limit of input force of +/-500N. To reduce the complexity of the optimization, control inputs are allowed to change every other step in the MPC horizon. The system parameters are kept the same as in previous sections, and state variables are initialized at rest with both pendula downwards. The controller is run at 100 Hz with a time horizon of .20 seconds. The APOPT solver is used as the default solver however, when this solver fails to converge, the IPOPT solver is used. Results of control over a one second interval is shown in figure 6.

The controller successfully balances the pendula upwards for a time before the high degree of nonlinearity near the desired equilibrium state render the system instantaneously uncontrollable. At this point, the controller begins to chatter as the sensitivities of the objective function to the

APMonitor		Objective	CV(1)	CV(2)	CV(3)	CV(4)	CV(5)
	Sensitivities	Function	p(35).n(3).x1	p(35).n(3).th1	p(35).n(3).th2	p(35).n(3).ojth1	p(35).n(3).ojth2
FV(1)	p(1).n(1).p1	0.00	0.816534	3.99263	-1.55816	-0.407077	0.511306
FV(2)	p(1).n(1).p2	0.00	0.200324	-0.215287	2.69655	0.017554	-1.21302
MV(1)	p(1).n(1).f	0.00	5.532E-04	1.295E-03	5.167E-04	-1.056E-04	-1.696E-04

Figure 5: Sensitivities near the unstable desired equilibrium point.

manipulated variable near this point begin to disappear. Sensitivities near the unstable equilibrium point are shown in figure 5.

The second pendulum eventually falls away from the desired set points as time progresses. Using different objective norms or weightings on objectives did not in this case improve control. It was found that despite the second pendulum falling away from the desired set point, sensitivities of the objective function to input force further vanished. In essence, the controller had fallen into a local minimum and would readily sacrifice the second pendulum's objective to keep the first at its desired set point. Longer horizons occasionally provided better control, however often solvers would fail to converge and resulting control would be sub-optimal. In short, the double pendulum system is an extremely difficult nonlinear system to control and using a linearized feedback system as shown in [2] may be more effective than MPC.

7 Conclusion

Simulation, estimation and control have been demonstrated on the double inverted pendulum in this paper. Simulation results match the expected behavior of the system, and results from the estimation demonstrate how moving horizon estimators can be used to determine unknown

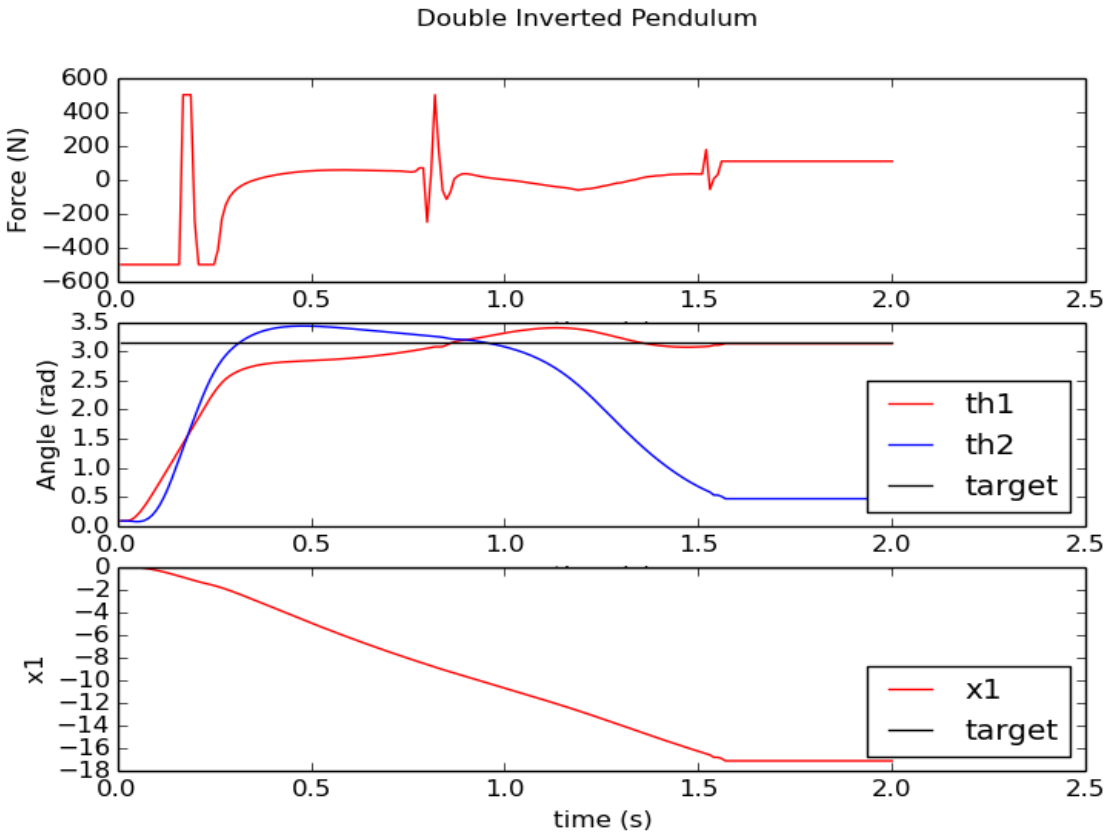

Figure 6: Sensitivities near the unstable desired equilibrium point.

parameters. Finally a controller is shown to temporarily balance the double inverted pendulum system about its unstable equilibrium point, before system nonlinearities and low sensitivities prevent accurate control.

References

[1] S. Jadlovská and J. Sarnovskỳ, "Classical double inverted penduluma complex overview of a system," in *Applied Machine Intelligence and Informatics (SAMI), 2012 IEEE 10th International Symposium on.* IEEE, 2012, pp. 103–108.

[2] M. Nalavade, M. J. Bhagat, and V. V. Patil, "Balancing double inverted pendulum on cart by

linearization technique," *International Journal of Recent Technology and Engineering (IJRTE), ISSN*, pp. 2277–3878.